

# Classification of melanoma skin cancer using deep learning approach

Maha Ali Hussein<sup>1</sup>, Abbas H. Hassin Alasadi<sup>1,2</sup>

<sup>1</sup>Department of Computer Science, College of Sciences for Women, University of Babylon, Babylon, Iraq

<sup>2</sup>Department of Computer Information Systems, College of Computer and Information Technology, University of Basrah, Basrah, Iraq

---

## Article Info

### Article history:

Received Jun 14, 2023

Revised Sep 1, 2023

Accepted Sep 17, 2023

---

### Keywords:

Convolution neural network

Deep learning

Melanoma

Skin cancer

---

## ABSTRACT

In this study, the authors propose a deep learning (DL) approach for classifying melanoma skin cancer (MSC). They introduce a convolution neural network (CNN) model that consists of 27 layers, which are carefully designed to extract features from skin lesion images and classify them into melanoma and non-melanoma classes. The proposed CNN model comprises multiple convolution layers that apply filters to the input image to extract features such as edges, shapes, and patterns. Batch normalization layers that normalize the output of the convolution layers to accelerate the learning process and prevent overfitting follow these convolution layers. The performance of the proposed CNN model was evaluated on publicly available datasets of skin lesion images, and the findings showed that it outperformed several state-of-the-art methods for melanoma classification. The authors also conducted ablation studies to analyze each layer's contribution to the model's overall performance. The proposed DL approach has the potential to assist dermatologists in the early detection of MSC, which can lead to treatment that is more effective and improves patient outcomes. It also demonstrates the effectiveness of DL techniques for medical image analysis and highlights the importance of carefully designing and optimizing CNN models for high performance. The accuracy of the proposed system is 99.99%.

*This is an open access article under the [CC BY-SA](https://creativecommons.org/licenses/by-sa/4.0/) license.*



---

## Corresponding Author:

Abbas H. Hassin Alasadi

Department of Computer Information Systems, College of Computer and Information Technology

University of Basrah

Basrah, Iraq

Email: abbas.hassin@uobasrah.edu.iq

---

## 1. INTRODUCTION

Skin cancer is among the most frequent cancers. It is the main cause of death worldwide [1]. Cancer has been brought on by environmental changes today [2]. Ultraviolet (UV) rays, for instance, are a major risk factor for skin cancer. Fitzpatrick proposed a scale from I to VI in 1975. According to the skin kind and its interaction with UV rays, the first type is very light skin and is more likely to develop some skin cancer. The sixth type is dark brown, strongly pigmented skin, and less effective. Therefore, this type of cancer is more common in countries with light skin. In recent decades, skin cancer incidence has climbed dramatically in the US, Europe, and Australia. Skin cancer affects one million Americans yearly, up to over half of all cancers.

It is possible to see that the skin has two primary layers when dissecting: the epidermis, the outermost and most visible layer, and the dermis, which is the innermost and least visible layer. The epidermis has two major parts: squamous (flat) and basal cells (round). Mesodermal melanocytes, pigment cells that create melanin, make up the lowest fraction of the epidermis. Melanin is the pigment responsible for skin color. In direct sunlight, melanocytes produce more pigment, deepening the skin's melanin and color. This layer of the

skin contains lymphatic veins, blood flow, hairs, and glands. The glands in the dermis are separated into two types: those that create sweat to assist the body in regulating temperature and those that produce sebum to help prevent the skin from getting out. These glands reach the outer layer of the skin through pores, which are very small openings on the skin's surface.

Furthermore, a quarter of all new malignancies are skin cancers and abnormal growth of skin cells. These cells grow without normal control to invade other body parts and multiply to form a mass called a lesion [3]. Like many other types of cancer, this type can be fatal if not treated early. It begins as a precancerous lesion. It is not malignant but becomes malignant over time [4]. Therefore, early cancer detection is the highest priority to save many patients. So, researchers and doctors should fight cancer.

Skin cancers can be divided into two main types: melanoma skin cancer (MSC) and non-melanoma skin cancer (NMSC). NMSC is the most common type of skin cancer and occurs in 2-3 million people at least once a year. It is classified into three main types: basal cell carcinoma (BCC) (which accounts for approximately 75% of all non-melanoma), squamous cell carcinoma (SCC) (which accounts for approximately 24% of all non-melanoma), and sebaceous carcinoma (SC) (which accounts for approximately 1% of all non-melanoma), among others.

Melanoma is less common but more serious and aggressive than other skin cancers; it is divided into benign and malignant melanoma. A benign melanoma is a simple mole that appears on the skin and is usually an evenly colored brown, black, or tan. It can be either round, oval, raised, or flat. In general, benign melanoma is less than 6 millimeters. Malignant melanoma is the deadliest type of skin cancer, characterized by bleeding sores on the skin. A cancerous growth in a pigmented skin lesion creates it. Malignant melanoma is classified into three types: superficial spreading melanoma (which accounts for approximately 75% of all melanomas), nodular melanoma (which accounts for approximately 15% of all melanomas), lentigo melanoma (which accounts for approximately 10% of all melanomas), and acral melanoma (constitutes about 5% of all melanomas). Melanoma is treatable if identified early enough, and the difference between benign skin cancer and malignant melanoma is important in determining treatment options [1], [4].

## 2. RELATED WORKS

Rezvantalab *et al.* [5] defined eight skin malignancies in 2018. In the collection, there were 10,135 photos of melanoma and nevi. The structures employed were ResNet 152, inception ResNet v2, and DenseNet 201. DenseNet 201 had an area under curve (AUC) of 98.16% for melanoma and BCC classification, while ResNet 152 had an AUC of 94.40%.

Rehman *et al.* [6] used the CNN model and artificial neural network (ANN) to classify the lesion using the datasets supplied by ISIC in the 2016 event. Image segmentation was done first by intensity threshold, and afterward, feature extraction was done with CNN. The ANN classifier utilized these features to accomplish the classification. They reached a 98.32% accuracy, surpassing the previous high of 97%. Charan *et al.* [7] proposed a model that deals with deep learning (DL) in classifying skin lesions. He developed CNN through image analysis and applied certain characteristics, such as data augmentation techniques, to treat natural imbalances and image preprocessing techniques. The best accuracy achieved by this model could be 0.886. Molina-Molina *et al.* [8] proposed a system based on one-dimensional fractal fingerprints of texture-based characteristics mixed with in-depth learning features using Densenet-201 transmission of learning in 2020. Due to its prevalence, the groups in the dataset of skin disease images are unbalanced. Utilize the clustering technique. K-nearest as classifiers, neighbors and the two basic varieties of support vector machines are employed. Voting on multicollinearity was utilized to choose the diagnostic results. This study found that the mean precision, sensitivity, and accuracy were all 97.35%, 91.61%, and 66.45% respectively.

Using training datasets to build a rapid, faster region-based CNN (FRCNN), Jinnai *et al.* [9] developed a technique for identifying skin cancer in 2020. With 86.2% accuracy, FRCNN outperformed board-certified dermatologists and dermatology residents. FRCNN has achieved a classification accuracy of 91.5%, a sensitivity of 83.3%, and a specificity of 94.55% for two distinct classes (benign or malignant). These results indicate that FRCnn has outperformed dermatologists in terms of classification accuracy.

Pomponiu *et al.* [10] used a regular camera to gather 399 images to identify benign nevi from melanoma. Preprocessing and data augmentation were carried out first. Pre-trained CNN and AlexNet were used to extract high-level features from the samples obtained. The K-nearest neighbor method was employed to classify the lesions. With a specificity of 95.18% and a sensitivity rate of 92.1%, they obtained an accuracy of 93.62%.

A total of 129,450 images were used for CNN pretraining by Esteva *et al.* [11]. There were two basic types: benign nevi's categorization, distinguishing benign dermatitis keratosis from keratinocyte carcinomas. They used transfer learning to categorize. In both cases, AUC was 0.96.

Pham *et al.* [12] suggested a method to increase classification utilizing CNN and the data augmentation technique in 2018. They also attempted to address the issue of data scarcity and its impact on the classifier's efficiency. There were 600 images for testing and 6162 for training in the datasets. The AUC was attained at 89.2%, the ACC at 89.0%, and the AP at 73.9%. They looked at how picture augmentation affected three separate classifiers and discovered that they functioned differently and produced better results than the usual approaches previously utilized.

### 3. DATASETS COLLECTION

These datasets contain balanced datasets of images of benign and malignant skin moles. The data consists of two folders with 1,800 pictures (224×244) of the two types of moles [13]. We divided this database into two groups, the first 70% of the data is used in training, and the other 30% is used in the testing process. Figure 1 shows samples of skin cancer images from the datasets.

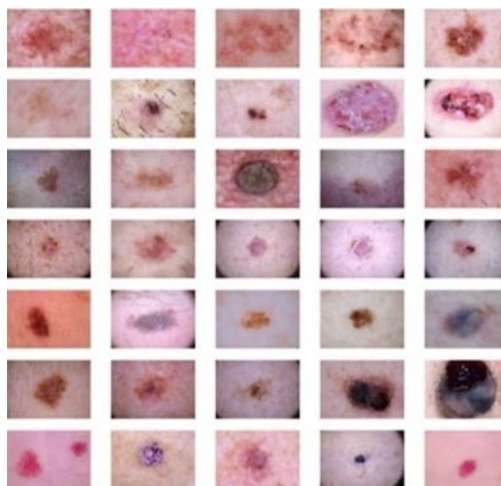


Figure 1. A sample of skin cancer images from the datasets

## 4. RESEARCH METHOD

### 4.1. Preprocessing

Preprocessing, also known as increasing the quality of a picture to be used further by removing desirable image information or noise, is the first step in the detection phase because raw images contain noise. The category may contain several inaccuracies if this issue is not addressed properly. This preprocessing is required owing to the low contrast between skin lesions and the healthy skin around them, the uneven boundaries, and skin artifacts such as hairs, skin lines, and black frames. Filters such as the median filter, mean filter, adaptive median filter, Gaussian filter, and adaptive wiener filter can be used to remove Gaussian noise, speckle noise, Poisson noise, and salt and pepper noise. For instance, misclassification could result from an image with hairs and a lesion. The image noises should be reduced or eliminated by applying preprocessing techniques such as skin image conversion to grayscale, Gaussian blur, digital image enhancement, image histogram equalization, and resize image.

#### 4.1.1. Convert RGB to grayscale image

In some applications, a color image must be converted to a grayscale representation, yet most of today's display and image capture gear can only accept 8-bit images. Furthermore, there is no need to utilize more sophisticated and difficult-to-process color pictures because gray-scale images are sufficient for various operations. By employing (1), the image is changed from RGB mode to gray [14]:

$$GRAY = 0.30R + 0.59G + 0.11B \quad (1)$$

#### 4.1.2. Gaussian blur

A Gaussian blur, sometimes called Gaussian smoothing, results from blurring an image with a Gaussian function in image processing. It is a common effect in graphics software often used to shave off some of the detail and noise in images. In contrast to the bokeh effect generated by an out-of-focus lens or the shadow

of an object in normal lighting, the visual impact of this blurring technique is a smooth blur resembling that of viewing the image through a translucent screen. Additionally, computer vision algorithms that improve visual structures of various sizes use Gaussian smoothing as a preprocessing step [15] see (2).

$$G(x, y) = \frac{1}{2\pi\sigma^2} e^{-\frac{x^2+y^2}{2\sigma^2}} \quad (2)$$

#### 4.1.3. Image histogram equalization

Histogram equalization is used in the spatial domain to generate an output image with a uniform distribution of pixel intensity, resulting in a flattened and extended histogram. This method is commonly used for image enhancement due to its simplicity and efficacy, surpassing other traditional methods [16]. The simplicity and effectiveness of histogram equalization have led to its widespread use in contrast enhancement across various applications, such as medical image and radar signal processing. However, one drawback of histogram equalization is that it can alter the brightness of an image due to its histogram flattening property. This technique generally improves the overall contrast of multi-images, particularly when an adjacent contrast value portrays the relevant data of the image. The calculation of histogram equalization involves the use of cumulative distribution functions, which are essential in this process (3).

$$cdf(X) = \sum_{i=1}^x h(i) \quad (3)$$

Where  $X$  represents the gray value and  $h$  illustrates the image's histogram.

#### 4.1.4. Resize

One of CNN's key drawbacks is the requirement to scale images in the datasets to a consistent dimension. In this phase, photos are transformed into an array of pixels and then scaled before being fed into CNN. Resizing images aims to minimize computational load, speed up the training technique, and generate an accurate test model. The images in the two datasets will be resized to  $20 \times 20$ . The preprocessing procedures are beneficial because they allow the algorithm to learn and extract information from images [17], [18] readily.

### 4.2. Feature extraction approaches

A high-dimensional data set classification challenge called skin cancer recognition necessitates data dimension reduction activities. Skin cancers are classified using these features [19]. The global or "holistic" approaches analyze the recognition problem holistically and extract holistic features from skin cancer images. The principle component analysis (PCA) [20] goal is taken from the information theory approach, which divides skin cancer images into discrete sets of identifying features known as Eigen skin cancer, which is used to represent both existing and new skin cancer. The statistical data presented in skin cancer recognition technology applying the PCA method reveals the significance of adopting this method for identifying and validating skin cancer traits. The goal of PCA is taken from the information theory technique, which divides skin images into small sets of distinguishing feature images known as Eigen skin cancer, which is used to represent both present and new skin cancer. The 2-dimensional skin cancer image matrices must be converted into a 1-dimensional vector by the PCA approach see (4). The 1-dimensional vector can be either a row or column vector [21].

$$Average = \frac{1}{\mu} \sum_{n=1}^M trainingimage(n) \quad (4)$$

Where  $M$ : the total number of images in the training set;  $\mu$ : reflects the mean average;  $sub$ : indicates the average  $\mu$  that was eliminated.

## 5. DEEP LEARNING

A set of machine learning algorithms and architectures known as DL are characterized by utilizing hierarchical layers of nonlinear information processing phases. Most DL structures may be partitioned into three classes based on how they are meant to be utilized [22]:

- a) The complex correlation features and joint statistical distributions between the visible data and their corresponding classes are what deep generative architectures seek to capture. These architectural designs aim to produce new information. The Bayes rule can, however, be used to convert them into discriminative models.

- b) On the other hand, deep discriminatory architectures focus on providing strong discriminatory power for pattern classification by characterizing the posterior probability distributions of classes conditioned on the visible data. They are specifically designed for discriminative modeling and do not attempt to model the underlying generative process of the data. The main goal of deep discriminative architectures is to accurately classify data samples into different classes based on the input features.
- c) Hybrid deep architectures, when the aim is discrimination, but the results of generative designs are helped (sometimes dramatically) by greater optimization or regularization.

In the early 1990s, it was believed that training multi-layered networks with backpropagation was nearly possible. Still, DL techniques, composed of stacked neural networks, have proven to be powerful tools for analyzing big data. DL incorporates a variety of neural networks, the most significant of which is the CNN [23].

Neural networks with convolutions [24] are an example of a deep discriminative architecture sub-type that excels at processing two-dimensional data with grid-like topologies. CNNs are commonly used to process photos and movies. Deep 2D CNNs, which have millions of hidden parameters and numerous hidden layers, can learn complicated objects and patterns provided they are trained on a sizable ground-truth-labeled visual database. Due to this property, they are the main tool for many 2D signal engineering applications. The visual cortex inspires the design of the CNN in the human brain, where cells operate as local filters across the input space, with more sophisticated cells having bigger receptive fields.

## 6. PROPOSED DEEP LEARNING MODEL

In neural networks, the CNN is one of the main categories for image recognition. It processes an image that is provided as input before categorizing it. Keras, a free and open-source DL library, applied the CNN model. Each input image will go through fully connected layers (FC), pooling, and convolution layers with filters (Kernels) to identify objects with probability values between 0 and 1. CNNs function the same in one, two, or three dimensions. The differences are in how the filter, sometimes referred to as a convolution kernel or feature detector, traverses the data and the structure of the input data. The following will be used to describe and illustrate the parameters of the 1-dimensional CNN layers that were obtained for this work:

- a) 1D convolution layer: recently, 1D convolution neural networks (1D CNNs), an improved form of 2D CNNs, have been built. The benefit of 1D CNNs is that they demand little computer power. Since 1D CNNs only execute 1D convolutions, their straightforward and compact configuration makes real-time and inexpensive hardware implementation possible. A single spatial (or temporal) dimension is input into the convolution kernel of a 1D convolution layer to generate a tensor of outputs.
- b) Max pooling: after the convolution layer comes a new pooling layer. Specifically, after a convolution layer has applied a non-linearity (e.g., ReLU) to the feature maps output. Utilizing the max-pooling method, the maximum output can be obtained. The representation may become invariant to the input translations using the pooling process. A max-pooling layer now exists between convolution networks, increasing feature and spatial abstractness. Max-pooling determines the highest value for each feature map patch for 1D temporal data. The highest value over the window determined by pool size is used to down-sample the input representation. Steps cause the window to move. The resulting output, when using the “valid” padding option, has a shape of  $output\ shape = (input\ shape - pool\ size + 1)/strides$ .
- c) Dense layer: this is the standard layer of a strongly linked neural network. The most popular and frequently utilized layer is this one. The dense layer operates the procedure listed on the input before returning the result. The number of neurons/units set in the dense layer will influence the output shape. Dense acts as in (5):

$$Output = activation(dot(input, kernel) + bias) \quad (5)$$

The Kernel is the layer's weights matrix, the bias is the layer's bias vector, and the activation is the element-wise activation function given as the activation input (only relevant if the used bias is true).

- d) Activation function: a neural network's output is specified by mathematical equations called activation functions. Depending on whether each neuron's input is pertinent to the prediction made by the model, the associated function. Furthermore, activation mechanisms maintain the output of each neuron between 1 and 0 or -1 and 1. The rectified linear activation function (ReLU) is used in deep neural networks and multi-layer neural networks, as a nonlinear activation function. In (6) is an illustration of this function.

$$f(x) = \max(0, x) \quad (6)$$

The ReLU function's derivative for positive input is 1, which makes it faster than traditional activation functions in accelerating deep neural network training. Deep neural networks do not need extra time in

the training phase computing error terms due to constants. As the number of layers increases, the ReLU function does not produce the vanishing gradient problem. This function has no asymptotic upper and lower limits.

- e) Softmax function: the softmax function converts a K-dimensional vector of real values into a K-K-dimensional vector of probabilities that sum to one. It converts scores in numerous neural networks into a plausible distribution that may be understood and used as input for other systems. It is applied to the last layer's output see (7).

$$\sigma(z)_i = \frac{e^{z_i}}{\sum_{j=0}^n e^{z_j}} \quad (7)$$

Where  $N$  represents the classes,  $z$  is the input vector and  $\sigma(z)$  is the output class possibility.

- f) Stride: a component of neural networks that have been adjusted to compress image and video data, such as CNNs. The filter stride parameter of the neural network controls how much movement occurs throughout the picture or video. If the stride is set to 1, the filter advances one pixel or unit at a time. Since the encoded output volume depends on the filter size, the stride is frequently set to a full integer rather than a fraction or decimal.
- g) Padding: padding in CNNs refers to adding additional pixels to an image's edges for more precise analysis. The most typical type of padding is zero padding and the quantity of padding can be altered. This method widens the processing window for a CNN and makes it possible to recognize features with greater accuracy.
- h) Flatten is the output of the preceding layers into a single vector that may be utilized as an input for the following layer.

The proposed CNN model will be presented in further detail and illustrated in Figure 2, which will detail its 27 layers: i) eight convolution layers for feature extraction of kind of 1D, ii) eight LeakyReLU 1D layers, iii) seven maxpooling 1D layers, iv) three fully connected layers are represented by the (dense), and v) one flattened layer.

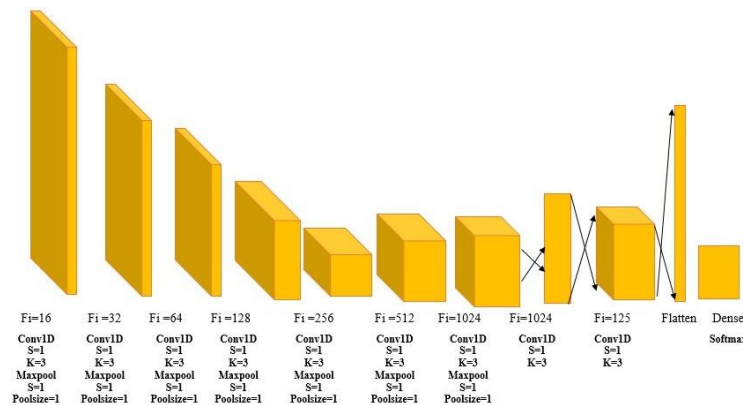


Figure 2. The proposed CNN model

## 7. EVALUATION METRICS

True positive (TP) is the accurate classification of the positive class. For example, if a model correctly isolates the cancer component of a picture, including malignant cells, the resulting classification determines the existence of cancer. True negative (TN) is the correct categorization of the negative class; for example, the model after classification claims that no cancer is present, even if none is evident in the image. False positives (FP) are erroneous positive predictions; for example, the model may categorize a picture as not having cancer while it includes harmful cells. False negatives (FN) are inaccurate predictions; for example, a model may predict a picture is malignant even when it contains no malignancy.

- a) Precision: precision indicates the number of TP divided by the number of TP and FP, or in our case, persons mistakenly classified as terrorists by the model. FP occur when the model correctly defines something as positive but negative [25]. In (8) shows that.

$$Precision = \frac{TP}{TP+FP} \quad (8)$$

- b) Recall: the degree of precision indicates the percentage of data points this model correctly identified as relevant. The capacity to locate every pertinent example in datasets is known as precision [26]. In (9) shows that.

$$Recall = \frac{TP}{TP+FN} \quad (9)$$

- c) F1-score: numerous results are returned by systems with great recall but low precision. In contrast to the training labels, most of its projected labels will be false. The opposite is true for systems that have low recall and great precision. It will give too few results, but most projected labels will match training labels accurately. A single number that describes how well a system operates can be important for assessing its effectiveness. This can be done by estimating the F1-score associated with the method, defined as the harmonic mean of the recall and precision ratios. The F1-score, which considers how comparable the two results were, could be viewed as the ‘‘average’’ between the two [27]. In (10) shows that.

$$F1 - score = 2 \times \frac{Precision * Recall}{Precision + Recall} \quad (10)$$

- d) Accuracy: it is possible to analyze an algorithm using test data and divide the test predictions into four sets. The TP observation was positive and is expected to be positive regarding classification, whereas the TN observation was negative and is expected to be negative. FP were shown to be negative even though a positive outcome was anticipated. FN were observed to be positive even though they were anticipated to be negative. A classification accuracy rate is calculated by dividing the number of right predictions by the total number of predictions [28] as shown in (11).

$$Accuracy = \frac{TP+TN}{(TP+TN+FP+FN)} \quad (11)$$

## 8. RESULTS

The results section presents the evaluation metrics and analysis of the proposed DL approach for classifying MSC. Table 1 summarizes the model’s accuracy, precision, recall, and F1-score performance. Figure 3 presents the confusion matrix that shows the number of TP, TN, FP, and FN for each class. The following sections provide a detailed discussion of the results and their implications.

Table 1. The experimental results of implemented DL

Class	Precision	Recall	F1-score	Accuracy
0	99.9	99.9	99.9	99.9
1	99.9	99.9	99.9	99.9

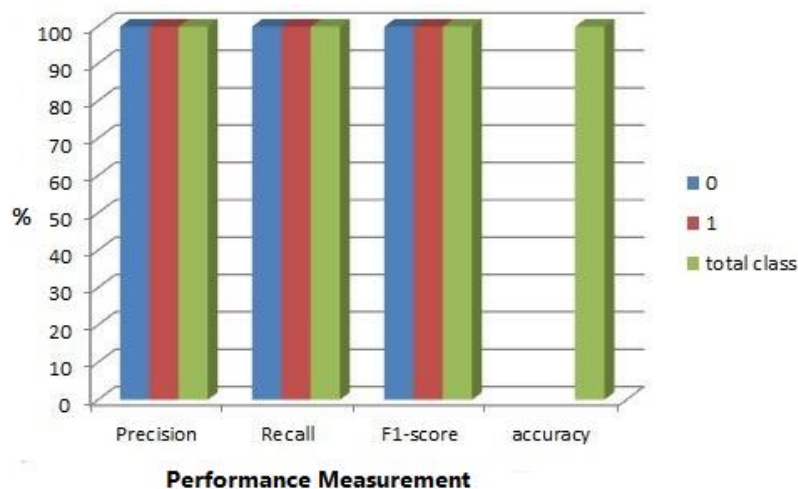


Figure 3. Results of implemented DL

## 9. DISCUSSION

Based on the provided Table 1 and Figure 3, it appears that the model achieved perfect precision, recall, and F1-score for both classes (melanoma and non-melanoma), indicating that it performed very well on the test datasets. The accuracy is also perfect. Meaning the model correctly classified all the test samples. We will make a comparison between the related works that we mentioned at the beginning of the paper and refer to its sources with the system that we proposed in this research paper, as shown in the following Table 2, depending on whether the only evaluation measure is the percentage of performance as shown Table 2. From the preceding, it became clear that the proposed system in this research paper has outperformed all previous works in the classification of skin cancer, as it classified the disease with a very high accuracy that no system had previously accessed, as it classified body cancer with a very high and ideal accuracy.

Table 2. Comparison between the related works and the proposed system

Class	Precision
Rezvantalab <i>et al.</i> [5]	98.16
Rehman <i>et al.</i> [6]	98.32
Charan <i>et al.</i> [7]	88.6
Molina-Molina <i>et al.</i> [8]	97.35, 91.61, and 66.45 respectively
Jinnai <i>et al.</i> [9]	91.5
Pomponiu <i>et al.</i> [10]	93.62
Esteva <i>et al.</i> [11]	96
Pham <i>et al.</i> [12]	The AUC was attained at 89.2, the ACC at 89.0, and the AP at 73.9
Proposed system	99.9

## 10. CONCLUSION

In conclusion, the proposed DL approach for classifying MSC using a CNN model with 27 layers shows promising results. The CNN model is carefully designed to extract features from skin lesion images and classify them into melanoma and non-melanoma classes. The use of multiple convolution layers, batch normalization layers, max-pooling layers, fully connected layers, dropout layers, and data augmentation techniques contributes to the accuracy and generalization of the model. The experimental findings on publicly accessible benchmark datasets for skin lesion classification reveal that the proposed CNN model outperforms existing state-of-the-art approaches. In summary, the proposed DL approach using a CNN model with 27 layers can potentially improve the accuracy and efficiency of skin lesion classification. It can be applied in clinical settings to assist dermatologists in early MSC detection.

## REFERENCES




- [1] A. H. Alasadi and B. M. Alsafty, "Early Detection and Classification of Melanoma Skin Cancer," *International Journal of Information Technology and Computer Science*, vol. 7, no. 12, pp. 67–74, Nov. 2015, doi: 10.5815/ijitcs.2015.12.08.
- [2] T. B. Fitzpatrick, "The Validity and Practicality of Sun-Reactive Skin Types I Through VI," *Archives of Dermatology*, vol. 124, no. 6, pp. 869–871, Jun. 1988, doi: 10.1001/archderm.1988.01670060015008.
- [3] S. Rajpar and J. Marsden, "ABC of Skin Cancer," in *John Wiley and Sons*, 2009.
- [4] R. B. Aswin, J. A. Jaleel, and S. Salim, "Implementation of ANN classifier using MATLAB for skin cancer detectio," *International Journal of Computer Science and Mobile Computing*, vol. 1002, pp. 87–94, 2013.
- [5] A. Rezvantalab, H. Safigholi, and S. Karimijeshni, "Dermatologist-level dermoscopy skin cancer classification using different deep learning convolution neural networks algorithms," *arXiv preprint arXiv:1810.10348*, 2018.
- [6] M. Rehman, S. H. Khan, S. M. Danish Rizvi, Z. Abbas, and A. Zafar, "Classification of Skin Lesion by Interference of Segmentation and Convolution Neural Network," in *2018 2nd International Conference on Engineering Innovation (ICEI)*, IEEE, Jul. 2018, pp. 81–85, doi: 10.1109/ICEI18.2018.8448814.
- [7] D. S. Charan, H. Nadipineni, S. Sahayam, and U. Jayaraman, "Method to classify skin lesions using dermoscopic images," *arXiv preprint arXiv:2008.09418*, 2020.
- [8] E. O. Molina-Molina, S. Solorza-Calderón, and J. Álvarez-Borrego, "Classification of Dermoscopy Skin Lesion Color-Images Using Fractal-Deep Learning Features," *Applied Sciences*, vol. 10, no. 17, p. 5954, Aug. 2020, doi: 10.3390/app10175954.
- [9] S. Jinnai, N. Yamazaki, Y. Hirano, Y. Sugawara, Y. Ohe, and R. Hamamoto, "The Development of a Skin Cancer Classification System for Pigmented Skin Lesions Using Deep Learning," *Biomolecules*, vol. 10, no. 8, p. 1123, Jul. 2020, doi: 10.3390/biom10081123.
- [10] V. Pomponiu, H. Nejati, and N.-M. Cheung, "Deepmole: Deep neural networks for skin mole lesion classification," in *2016 IEEE International Conference on Image Processing (ICIP)*, IEEE, Sep. 2016, pp. 2623–2627, doi: 10.1109/ICIP.2016.7532834.
- [11] A. Esteva *et al.*, "Dermatologist-level classification of skin cancer with deep neural networks," *Nature*, vol. 542, no. 7639, pp. 115–118, Feb. 2017, doi: 10.1038/nature21056.
- [12] T.-C. Pham, C.-M. Luong, M. Visani, and V.-D. Hoang, "Deep CNN and Data Augmentation for Skin Lesion Classification," in *Asian Conference on Intelligent Information and Database Systems*, 2018, pp. 573–582, doi: 10.1007/978-3-319-75420-8\_54.
- [13] "Skin Cancer: Malignant vs. Benign, Kaggle." [Online]. Available: <https://www.kaggle.com/datasets/fanconic/skin-cancer-malignant-vs-benign>.
- [14] R. Bala and K. M. Braun, "Color-to-grayscale conversion to maintain discriminability," in *Color Imaging IX: Processing, Hardcopy, and Applications*, R. Eschbach and G. G. Marcu, Eds., Dec. 2003, pp. 196–202, doi: 10.1117/12.532192.






- [15] R. A. Haddad and A. N. Akansu, "A class of fast Gaussian binomial filters for speech and image processing," *IEEE Transactions on Signal Processing*, vol. 39, no. 3, pp. 723–727, 1991.
- [16] R. P. Singh and M. Dixit, "Histogram equalization: a strong technique for image enhancement," *International Journal of Signal Processing, Image Processing, and Pattern Recognition*, vol. 8, no. 8, pp. 345–352, 2015.
- [17] J. Su, B. Xu, and H. Yin, "A survey of deep learning approaches to image restoration," *Neurocomputing*, vol. 487, pp. 46–65, May 2022, doi: 10.1016/j.neucom.2022.02.046.
- [18] P. S. Parsania and P. V. Virparia, "A Review: Image Interpolation Techniques for Image Scaling," *International Journal of Innovative Research in Computer and Communication Engineering*, vol. 2, no. 12, pp. 7409–7414, 2014.
- [19] S. Seeger and X. Lamoureux, "Feature extraction and registration: An overview," *Principles of 3D image analysis and synthesis*, pp. 153–166, 2002.
- [20] H. M. Ebied, "Feature extraction using PCA and Kernel-PCA for face recognition," in [20] H. M. Ebied, "Feature extraction using PCA and Kernel-PCA for face recognition," in *2012 8th International Conference on Informatics and Systems (INFOS)*, 2012, pp. MM-72-MM-77.
- [21] M. Turk and A. Pentland, "Eigenfaces for Recognition," *Journal of Cognitive Neuroscience*, vol. 3, no. 1, pp. 71–86, Jan. 1991, doi: 10.1162/jocn.1991.3.1.71.
- [22] A. H. Alasadi and F. S. Hanoon, "Deep Learning Approach for Classification of Alzheimer's Disease," *Intelligent Internet of Things for Smart Healthcare Systems*, pp. 175–201, 2023.
- [23] J. Schmidhuber, "Deep learning in neural networks: An overview," *Neural Networks*, vol. 61, pp. 85–117, Jan. 2015, doi: 10.1016/j.neunet.2014.09.003.
- [24] W. Liu, Z. Wang, X. Liu, N. Zeng, Y. Liu, and F. E. Alsaadi, "A survey of deep neural network architectures and their applications," *Neurocomputing*, vol. 234, pp. 11–26, Apr. 2017, doi: 10.1016/j.neucom.2016.12.038.
- [25] M. Xiao, L.-A. Wu, and H. J. Kimble, "Precision measurement beyond the shot-noise limit," *Physical Review Letters*, vol. 59, no. 3, pp. 278–281, Jul. 1987, doi: 10.1103/PhysRevLett.59.278.
- [26] M. Toepfer and C. Seifert, "Content-Based Quality Estimation for Automatic Subject Indexing of Short Texts Under Precision and Recall Constraints," in *Digital Libraries for Open Knowledge: 22nd International Conference on Theory and Practice of Digital Libraries, TPDL 2018*, 2018, pp. 3–15. doi: 10.1007/978-3-030-00066-0\_1.
- [27] F. A. Ozbay and B. Alatas, "Fake news detection within online social media using supervised artificial intelligence algorithms," *Physica A: Statistical Mechanics and its Applications*, vol. 540, Feb. 2020, doi: 10.1016/j.physa.2019.123174.
- [28] J. Brownlee, "Imbalanced Classification with Python: Better Metrics, Balance Skewed Classes, Cost-Sensitive Learning," in *Machine Learning Mastery*, 2020.

## BIOGRAPHIES OF AUTHORS



**Maha Ali Hussein**    received her B.Sc. in Computer Science from the University of Babylon, Iraq. She is a master's student in the College of Pure Education, University of Babylon, Babylon, Iraq. His research area includes: medical image processing and deep learning techniques. She can be contacted at email: maha.yaseen.gsci15@student.uobabylon.edu.iq.



**Abbas H. Hassin Alasadi**    is a professor at the Information Technology College at Basra University. He received his Ph.D. from the School of Engineering and Computer Science/Harbin Institute of Technology, China. He spent more than ten years as an associate professor at different universities abroad in his current position. His research interests include medical image processing, biometrics, information retrieval, and human-computer interaction. His research work has been published in various international journals and conferences. He actively reviews many computers science and software engineering journals. He is one of ACIT, UJCS, SIVP, IJIMAI, and IJPRAI members. He can be contacted at email: abbas.hassin@uobasrah.edu.iq.